RESEARCH ARTICLE

Retinal Architecture in Autosomal Recessive Spastic Ataxia of Charlevoix-Saguenay (ARSACS): Insights into Disease Pathogenesis and Biomarkers

Flávio Moura Rezende Filho, MD,[1] Fion Bremner, MD, PhD,[2] José Luiz Pedroso, MD, PhD,[1*] João Brainer Clares de Andrade, MD, PhD,[1] Bruna Ferraço Marianelli, MD,[3] Charles Marques Lourenço, MD, PhD,[5] Wilson Marques-Júnior, MD, PhD,[5] Marcondes C. França, Jr., MD, PhD,[4] Fernando Kok, MD, PhD,[6,7] Juliana M.F. Sallum, MD, PhD,[3] Michael H. Parkinson, PhD, MBBS,[8] Orlando G. Barsottini, MD, PhD,[1] and Paola Giunti, MD, PhD[8*]

[1]*Division of General Neurology and Ataxia Unit, Department of Neurology, Universidade Federal de São Paulo, Sao Paulo, Brazil*
[2]*Department of Neuro-Ophthalmology, National Hospital for Neurology & Neurosurgery, London, UK*
[3]*Department of Ophthalmology, Universidade Federal de São Paulo, Sao Paulo, Brazil*
[4]*Department of Neurology, Universidade Estadual de Campinas, Campinas, Brazil*
[5]*Department of Neurology, University of São Paulo, School of Medicine, Ribeirão Preto, Brazil*
[6]*Mendelics Genomic Analysis, São Paulo, Brazil*
[7]*Department of Neurology, University of São Paulo, School of Medicine, São Paulo, Brazil*
[8]*Department of Clinical and Movement Neurosciences, Ataxia Centre, UCL, Queen Square Institute of Neurology, London, UK*

ABSTRACT: Background: Autosomal recessive spastic ataxia of Charlevoix-Saguenay (ARSACS) causes unique retinal abnormalities, which have not been systematically investigated.
Objective: To deeply phenotype the retina in ARSACS in order to better understand its pathogenesis and identify potential biomarkers.
Methods: We evaluated 29 patients with ARSACS, 66 with spinocerebellar ataxia (SCA), 38 with autosomal recessive cerebellar ataxia (ATX), 22 with hereditary spastic paraplegia (SPG), 21 cases of papilledema, and 20 healthy controls (total n = 196 subjects). Participants underwent visual acuity assessment, intraocular pressure measurement, fundoscopy, and macular and peripapillary optical coherence tomography (OCT). Macular layers thicknesses in ARSACS were compared with those of age-matched healthy controls. Ophthalmologists analyzed the scans for abnormal signs in the different patient groups. Linear regression analysis was conducted to look for associations between retinal changes and age, age at onset, disease duration, and Scale for the Assessment and Rating of Ataxia (SARA) scores in ARSACS.
Results: Only patients with ARSACS exhibited peripapillary retinal striations (82%) on fundoscopy, and their OCT scans revealed foveal hypoplasia (100%), sawtooth appearance (89%), papillomacular fold (86%), and macular microcysts (18%). Average peripapillary retinal nerve fiber layer (pRNFL) was thicker in ARSACS than in SCA, ATX, SPG, and controls; a cut-off of 121 μm was 100% accurate in diagnosing ARSACS. All macular layers were thicker in ARSACS when compared to healthy controls. RNFL thickness in the inferior sector of the macula positively correlated with SARA scores.
Conclusions: Retinal abnormalities are highly specific for ARSACS, and suggest retinal hyperplasia due to abnormal retinal development. OCT may provide potential biomarkers for future clinical trials. © 2021 International Parkinson and Movement Disorder Society

Key Words: optical coherence tomography; autosomal recessive spastic ataxia of Charlevoix-Saguenay; ARSACS; retina; ataxia

*__Correspondence to:__ Dr. José Luiz Pedroso, Department of Neurology, Universidade Federal de São Paulo, Sao Paulo, Brazil; E-mail: jlpedroso.neuro@gmail.com; Dr. Paola Giunti, Ataxia Centre, Queen Square Institute of Neurology, UCL/UCLH, Queen Square, London, UK; E-mail: p.giunti@ucl.ac.uk

Flávio Moura Rezende Filho, Fion Bremner, and José Luiz Pedroso contributed equally to this work.

Relevant conflicts of interest/financial disclosures: The authors have no conflicts of interest to report.

Funding agency: This research did not receive funding.

Received: 5 January 2021; **Revised:** 1 March 2021; **Accepted:** 15 March 2021

Published online 23 April 2021 in Wiley Online Library (wileyonlinelibrary.com). DOI: 10.1002/mds.28612

Autosomal recessive spastic ataxia of Charlevoix-Saguenay (ARSACS; OMIM 270550) is a neurodegenerative disease comprising cerebellar ataxia, spasticity, and peripheral neuropathy.[1] In 2000, researchers identified its causative gene, *SACS*, on chromosome 13q12.12.[2] This allowed molecular confirmation of ARSACS[3-7] revealing it as an important cause of autosomal recessive ataxia, possibly second only to Friedreich's ataxia in frequency.[8]

All ARSACS patients in the original published series exhibited increased visibility of the retinal nerve fibers on fundoscopy.[1] Further assessment using optic coherence tomography (OCT) showed thickening of the peripapillary retinal nerve fiber layer (pRNFL).[9,10] pRNFL thickening is usually seen in conditions associated with optic disc edema, including ischemic or inflammatory optic neuropathies and papilledema.[11-13] However, in ARSACS the optic disc is not swollen, and the pathogenesis of the pRNFL thickening remains unknown. Axonal edema[14,15] or hyperplasia[16,17] have been proposed as possible mechanisms, but to date no pathological report of a retinal specimen from a patient with ARSACS has been published. Although specific ocular phenotypes are seen in several forms of neurogenetic disorders displaying ataxia (eg, optic atrophy in ATX-*FXN*, fundus flavimaculatus-like in SPG11,[18] and cone–rod dystrophy in SCA7[19]), pRNFL thickening appears to be unique to ARSACS and is not seen in other conditions.[6]

In addition to pRNFL thickening, other retinal changes have been described. These include abnormal foveal morphology (interpreted either as thickening of the inner retinal layers[9,14] or as foveal hypoplasia[20]) and prominent vascular tortuosity.[3] A Brazilian study also reported papillomacular retinal folds, and a dentate appearance in the outer retina and macular microcysts.[7] Fovea-to-disc distance (FDD) is known to influence retinal architecture,[21,22] but it has not been investigated in ARSACS.

The prevalence of these various retinal architecture abnormalities in ARSACS, and their specificity to this type of ataxia, are unknown. In this study we have used spectral domain OCT (SD-OCT) to achieve both quantitative and qualitative retinal architecture analysis in 28 patients with molecularly confirmed ARSACS. We compared these results with those obtained from age-matched healthy controls, patients with other inherited ataxias, and patients with papilledema to identify which of these changes are unique to ARSACS. We use these data to draw tentative conclusions regarding the pathogenesis of ARSACS, and to identify potential biomarkers for future clinical treatment trials.

Patients and Methods

Study Participants

Subjects were recruited from 2008 to 2019 at the Ataxia Centre of the National Hospital for Neurology and Neurosurgery (London, UK), and from the Neurology and Neurosurgery Department of the Federal University of São Paulo (Brazil). The London Brent Research Ethics Committee and the Ethics Committee of the Federal University of São Paulo approved this study (reference codes 12/LO/1291 and 61538516. 9.0000.5505, respectively), which complied with the Declaration of Helsinki. We assessed 196 individuals: 29 patients with molecularly confirmed ARSACS; 126 patients with other hereditary ataxias or spastic paraplegias (66 autosomal dominantly inherited spinocerebellar ataxias [SCA], 38 autosomal recessive cerebellar ataxias [ATX], and 22 hereditary spastic paraplegias [(SPGs]); 20 age-matched healthy controls; and 21 patients with papilledema. All patients (or legal guardians) and healthy controls gave informed consent.

All participants had measurements of best-corrected visual acuity and intraocular pressure, and underwent fundoscopy. In the ARSACS cases, age at onset, disease duration, and Scale of the Assessment and Rating of Ataxia (SARA) score were recorded.

The exclusion criteria were: any other disease affecting retinal architecture, intraocular pressure greater than 20 mm Hg, cup-to-disc ratio >0.5, high refractive errors (±5 diopters equivalent sphere or ±2 diopters astigmatism), and ocular media opacities precluding examination.

Retinal Imaging

This study followed APOSTEL[23] and OSCAR-IB[24] recommendations for OCT studies. Retinal color pictures were taken using standard fundus cameras. Under dim light and cycloplegia, 870 nm SD-OCT devices (Spectralis, Heidelberg Engineering, software version 6.8.1, Heidelberg, Germany) acquired peripapillary circular B-scans (3.5 mm in diameter) to measure RNFL thickness in superior, inferior, nasal, and temporal quadrants, and calculate average RNFL thickness. The devices also obtained 25 macular horizontal B scans comprising 768 A scans each (15.77 mm^2 area, axial resolution of 3.87 μm/pixel). Foveal hypoplasia was graded using the system proposed by Thomas,[25] and vascular tortuosity, papillomacular fold, and sawtooth appearances were classified as absent, mild, or severe. RNFL thickness was defined as abnormal if greater than the 95th percentile of the Spectralis proprietary normative databank. Papilledema was graded using the Frisèn scale.

We used ImageJ (available at http://rsbweb.nih.gov/ij/; www.nih.gov, National Institutes of Health, Bethesda, MD), to measure the distance from the fovea to the optic disc center (FDD) in Spectralis® red-free fundus photographs. A rectangle fitting to the height and width of the optic disc was drawn, and the point of intersection of the rectangle diagonals defined the disc

center. The fovea was located using the foveal reflex on fundus photographs and the foveal pit, outer nuclear layer (ONL) widening and/or lengthening of the photoreceptors external segment on OCT imaging.

Segmentation of the Retinal Layers on OCT Images

Automated retinal segmentation (right eye) using Orion™ software (Voxeleron LLC, Pleasanton, CA) was performed in 20 patients with ARSACS and 20 age-matched healthy controls, and then manually checked by an ophthalmologist (J.M.F.S.). The software subsequently measured the thickness of the following seven layers in each sector of the macular Early Treatment Diabetic Retinopathy Study (ETDRS) grid (concentric ring diameters of 1, 3, and 6 mm): RNFL, ganglion cell layer-inner plexiform layer (GC-IPL), inner nuclear layer (INL), outer plexiform layer (OPL), ONL, photoreceptor layer (PR), and retinal pigmented epithelium/Bruch membrane (RPE-BRU). We excluded all ETDRS sectors in which retinal segmentation could be affected by sawtooth appearance, which prevented automated and manual layer demarcation. Thus the outer ETDRS ring was not evaluated and macular outcome measures were only obtained from the inner circle of the ETDRS map (IC-ETDRS). A detailed description of this procedure can be found in supplementary materials.

Statistical Analysis

We used IBM SPSS Statistics for Windows, version 21.0 (IBM Corp., Armonk, NY, 2012) and Microsoft Excel (2010) for statistical analysis. Differences between ARSACS and healthy controls in age, sex, pRNFL, and macular layers thicknesses were evaluated employing Student's *t* test (normal distribution) or Mann–Whitney U test (non-normal distribution). We applied analysis of covariance (ANCOVA) and Bonferroni correction in the comparison of average pRNFL and macular measurements in the different patient groups and healthy controls. Associations of retinal measurements (average pRNFL and macular layers thicknesses) and retinal findings (grade of vascular tortuosity, papillomacular fold, sawtooth appearance, foveal hypoplasia) with age, age at onset, disease duration, and SARA scores were sought using linear regression and ordinal regression, respectively. Age-adjusted correlations were also determined applying linear regression. Spearman correlation coefficient assessed the association between retinal layer thicknesses and qualitative abnormalities of different grades.

Results

Participants

We excluded one patient with ARSACS (dense cataracts) and another with SCA3 (chorioretinitis). The remaining 194 participants underwent the full study protocol. Details of the number of participants in each comparator group and their ages are shown in Table S1. There was no significant mean age difference between ARSACS and any of the remaining groups, but participants with SCA were older than those with ATX (ANOVA $P < 0.05$) and SPG (ANOVA $P < 0.01$).

Among the 28 (11 women) ARSACS patients, age at onset ranged from 1 to 48 (mean 14.5 ± 18.6) years, and disease duration from 9 to 44 (mean 24.5 $\pm$ 10) years. Sixteen individuals had their first symptoms within the first decade of life (64%). SARA scores varied from 5 to 26 (mean 12.5 ± 5.9). All cases had gait difficulty as the presenting feature, and disclosed cerebellar ataxia, lower limb spasticity, and signs of peripheral neuropathy. The 21 participants with papilledema had disc swelling judged as Frisen grade 2 in 8 patients, grade 3 in 5, grade 4 in 13, and grade 5 in four patients. The cohort of healthy control subjects (N = 20, 13 women) were recruited from the medical staff of the Neurology and Ophthalmology Departments of the Federal University of São Paulo.

Ophthalmological Evaluation

In both eyes of all participants visual acuity was 6/9 or better, intraocular pressure ranged from 8 to 18 mm Hg, and there were no abnormalities in anterior segment biomicroscopy. Fundus examination findings in ARSACS patients are described below. Apart from optic atrophy in the Friedreich's ataxia cohort and optic disc swelling in the papilledema cohort, fundus examination was unremarkable in all non-ARSACS participants.

Qualitative Analysis of Retinal Architecture

Fundoscopy

Twenty-three patients with ARSACS (82%) had increased visibility of retinal nerve fibers on fundoscopy, which was more prominent near the optic disc and along the superotemporal and inferotemporal arcades (Figure S1). Abnormal vascular tortuosity occurred in 19 patients with ARSACS (68%), appearing in all four quadrants but most apparent in the proximal third of the temporal arcades (arteries more than veins); it was graded as mild in 14 (74%) and severe in 5 (26%) individuals.

OCT

Foveal hypoplasia, as defined by the incursion of inner retinal layers anterior to the foveola, occurred in all eyes (100%) of ARSACS patients (half had grade 1, the other half grade 2) (Fig. 1). Twenty-five of these patients (89%) also exhibited a "sawtooth" appearance of pointed folds involving the inner nuclear, outer plexiform, and ONLs adjacent to the temporal sector of the optic disc; this was graded as mild (indentations < 1/3 of total retinal thickness) in 12 (43%) individuals, and gross (indentations > 1/3 of total retinal thickness) in 13 (46%) patients. A radial "papillomacular" fold was identified in the area between the fovea and optic disc in 24 cases (86%), which was most easily observed in OCT 3D reconstructions of the macula or in the peripapillary circular scans. This fold consisted of thickened inner retinal layers, and was graded as absent in four patients (14%), mild (height < 1/4 of total retinal thickness) in 12 patients (43%), and gross (height > 1/4 of total retinal thickness) in 12 patients (43%). Five patients (18%) from three different families had bilateral macular microcysts, consisting of round/oval-shaped hyporeflective spaces measuring 50–170 μm in their longest axis and visible in two or more adjacent scans. These microcysts were located both within the inner nuclear and ganglion cell layers in four patients but only in the INL in one patient. We performed follow-up OCTs in seven patients with ARSACS (after 3–5 years) and found no qualitative changes in their retinal architecture over time.

In contrast to the ARSACS group, fundoscopy and OCT in the SCA, ATX, and SPG groups did not reveal any patients with the findings described above. Five cases of papilledema exhibited macular microcysts exclusively in the INL and seven had retinal folds – but mostly annular rather than radial ('Paton's lines'), peripapillary, and affecting predominantly the RNFL (six cases). One eye with papilledema had choroidal folds and another had folds extending from the INL to RPE, but they did not resemble the sawtooth morphology found in ARSACS. No case of papilledema had absence of the foveal depression or a radial papillomacular fold.

Quantitative Analysis of Retinal Architecture

pRNFL

All ARSACS participants had thickened pRNFL. The average pRNFL ranged from 122 to 231 (mean 174.44) μm (Fig. 2). A pRNFL thickness above the Spectralis databank's 95th percentile occurred most often in the nasal (93%), followed by the inferior (81%), superior, and temporal (74% each) sectors. In 63% of patients all sectors were abnormally thickened. Supplementary Table S1 provides average pRNFL thickness for all comparator groups. Age-adjusted ANCOVA with Bonferroni correction for multiple tests (see Table 1) showed that the mean average pRNFL: (1) was thicker in ARSACS in comparison to all other groups ($P < 0{,}001$) and (2) was thinner in the ATX group when compared to normal controls ($P < 0.001$) and to SCA ($P < 0.05$) groups. The lowest value for average pRNFL thickness in ARSACS patients (122 μm) was higher than the highest value for average pRNFL found in any other group, providing an absolute differentiation between ARSACS, other neurogenetic disorders, and controls. Sectoral pRNFL thickness measurements in ARSACS overlapped the ranges of the other groups, and were less accurate in diagnosing ARSACS than average pRNFL.

FDD and Macular Measurements in ARSACS Versus Age-Matched Healthy Controls

A summary of FDD and macular measurements in both cohorts is shown in Table S2. FDD was significantly shorter ($P < 0.001$) in patients with ARSACS than in healthy controls. The differences between total macular thickness in patients with ARSACS and age-matched controls were significant for all sectors of the IC-ETDRS, except the temporal sector. All retinal layers in the nasal sector (except for RPE-BM) were thicker in ARSACS; in the foveal subfield, all layers were thicker apart from ONL and RPE-BM. All differences mentioned above remained significant after FDD-adjusted ANCOVA using Bonferroni correction ($P < 0.001$).

Regression Analysis

Among participants with ARSACS, age and age at onset correlated negatively with average pRNFL and with all averages of macular layers apart from OPL, PR, and BM (ie, the youngest patients had the greatest degree of abnormal retinal layer thickening) (Fig. 3). There were no significant associations between SARA scores or disease duration with macular or pRNFL measurements on linear regression. However, after adjusting for age, inferior RNFL showed a positive correlation with SARA scores.

FDD directly correlated with age and inversely correlated with the grades of papillomacular folds, sawtooth appearance and vascular tortuosity, mean nasal total macular thickness, and the average total retinal thickness. FDD inversely correlated with average pRNFL among healthy controls, but not in ARSACS. There was no significant association of FDD with SARA, age at onset, or disease duration.

The grade of sawtooth appearance and papillomacular fold exhibited an inverse correlation with age and age at onset, but no association with SARA or disease duration. Vascular tortuosity inversely correlated with age at onset. The grade of papillomacular folds and sawtooth appearance positively correlated with average pRNFL, temporal pRNFL, average total macular thickness, and nasal total macular thickness. Foveal hypoplasia grade did not

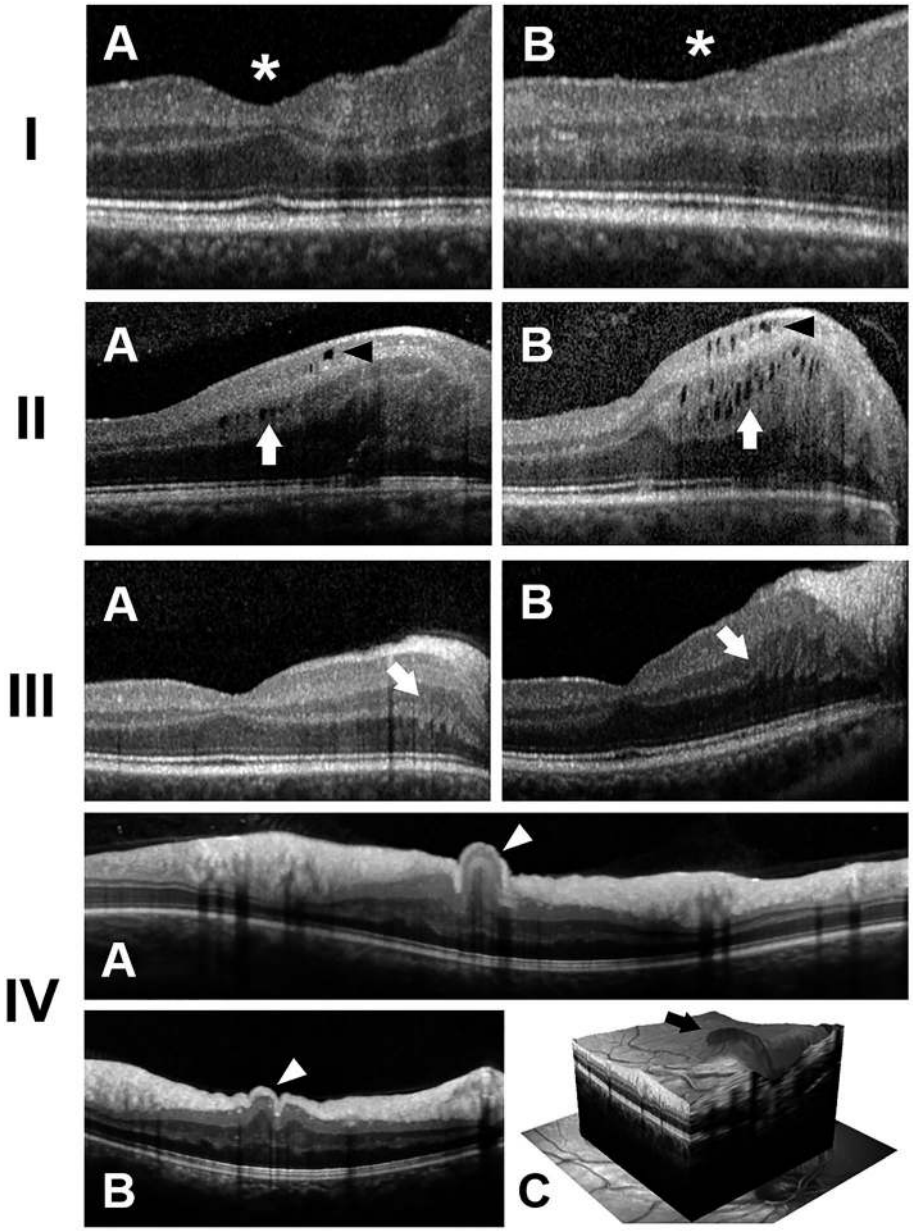

FIG. 1. Optical coherence tomography **(**OCT) findings in autosomal recessive spastic ataxia of Charlevoix-Saguenay (ARSACS). **I**. Foveal hypoplasia, as defined by the incursion of inner retinal layers anterior to the foveola, whose location is confirmed by the widening of outer nuclear layer (ONL) and lengthening of external segment of photoreceptors (asterisk). Horizontal macular B-scans (right eye) depict partial absence of foveal pit in an 18-year-old man, indicating grade 1 foveal hypoplasia (**IA**), and complete absence of foveal pit in a 30-year-old man, implying grade 2 (**IB**). **II**. Horizontal macular B-scans (right eye) showing macular microcysts, which consist of hyporeflective round or oval-shaped lesions located in the ganglion cell layer (arrowhead) and in the inner nuclear layer (INL) (arrow). The scans are from a 26-year-old woman (**IIA**) and her 30-year-old brother (**IIB**). **III**. Horizontal macular B-scans (right eye) disclosing pointed retinal folds involving the INL, outer plexiform layer (OPL), and ONL close to the temporal edge of the optic disc, which create a sawtooth appearance. This abnormality was mild in a 32-year-old woman (**IIIA**) and gross in a 16-year-old woman (**IIIB**). **IV**. The papillomacular fold, consisting of thickened inner retinal layers, is seen in the temporal region of peripapillary circular scans (white arrowheads). It was gross in a 21-year-old man (**IVA**) and mild in a 31-year-old man (**IVB**), and is clearly seen on Spectralis® 3D reconstruction of retinal tissue (arrow; **IVC**).

associate with average macular measurements or average pRNFL.

Discussion

We have analyzed retinal architecture in 28 patients with ARSACS, the largest series published to date. The classical fundoscopic finding of increased visibility of retinal fibers[1] occurred in 82% of our cohort, but pRNFL thickening in SD-OCT affected all individuals confirming the superiority of SD-OCT in the evaluation of suspected ARSACS cases. We also segmented macular scans to evaluate the thickness of other retinal layers in ARSACS cases and in 20 age-matched healthy

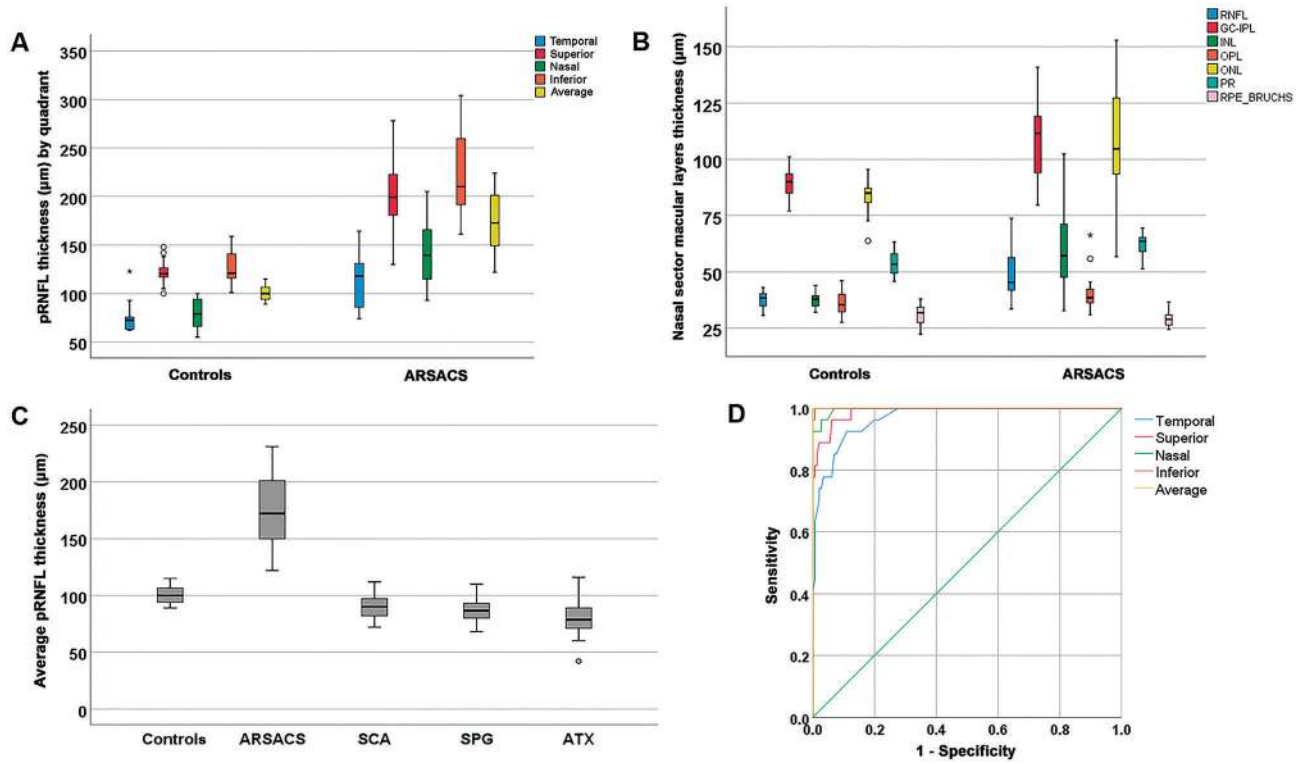

FIG. 2. Quantitative analysis of retinal architecture and diagnostic accuracy of peripapillary retinal nerve fiber layer (pRNFL). **A**. pRNFL thickness by quadrant and average pRNFL in autosomal recessive spastic ataxia of Charlevoix-Saguenay (ARSACS) and age-matched controls. **B**. Box-and-whisker plots of macular layers thicknesses in the nasal sector of the inner circle of the Early Treatment Diabetic Retinopathy Study (IC-ETDRS) map in ARSACS and age-matched controls. **C**. Box-and-whisker plots of average optical coherence tomography **(**OCT) measurements of pRNFL thickness in healthy controls, ARSACS, SCAs, SPGs, and autosomal recessive cerebellar ataxias (ATXs). **D**. Receiver operating characteristic curves representing the accuracy of each quadrant of pRNFL measurement and average pRNFL in differentiating ARSACS from SCAs, SPGs, and other ATXs. pRNFL, peripapillary retinal nerve fiber layer; ARSACS, autosomal recessive spastic ataxia of Charlevoix-Saguenay; SCA, spinocerebellar ataxia; SPG, hereditary spastic paraplegia; ATX, recessive ataxia.

TABLE 1 *P values for ANCOVA adjusted for age with Bonferroni correction in the comparison of average peripapillary retinal nerve fiber layer (pRNFL) in autosomal recessive spastic ataxia of Charlevoix-Saguenay (ARSACS), other neurogenetic disorders, and controls*

	ARSACS	SCA	SPG	ATX	Controls
ARSACS	–	<0.001	<0.001	<0.001	<0.001
SCA		–	1.0	0.036	0.339
SPG			–	1.0	0.09
ATX				–	<0.001
Controls					–

ARSACS, autosomal recessive spastic ataxia of Charlevoix-Saguenay; SCA, spinocerebellar ataxia; SPG, hereditary spastic paraplegia; ATX, autosomal recessive ataxia.

controls, as there is no normative database for these measurements. Our results show that the abnormal thickening is not confined to the RNFL but affects *all* retinal layers in ARSACS. Although some measurements in particular sectors and layers were normal, all patients with ARSACS showed abnormal thickening of all retinal layers in at least one sector of the IC-ETDRS. OCT has also revealed other retinal changes occurring at different frequencies in our cohort: foveal hypoplasia in 100%, sawtooth appearance in 89%, papillomacular fold in 86%, vascular tortuosity in 68%, and macular microcysts in 18%.

To determine the specificity of these retinal changes, we investigated patients with other types of inherited ataxia, SPG, and papilledema. In contrast to ARSACS, none of the patients with other neurogenetic conditions had any of the retinal abnormalities mentioned above. Participants with ARSACS also exhibited average pRNFL measurements invariably greater than 121 µm, while all those with other hereditary ataxias, SPG, or

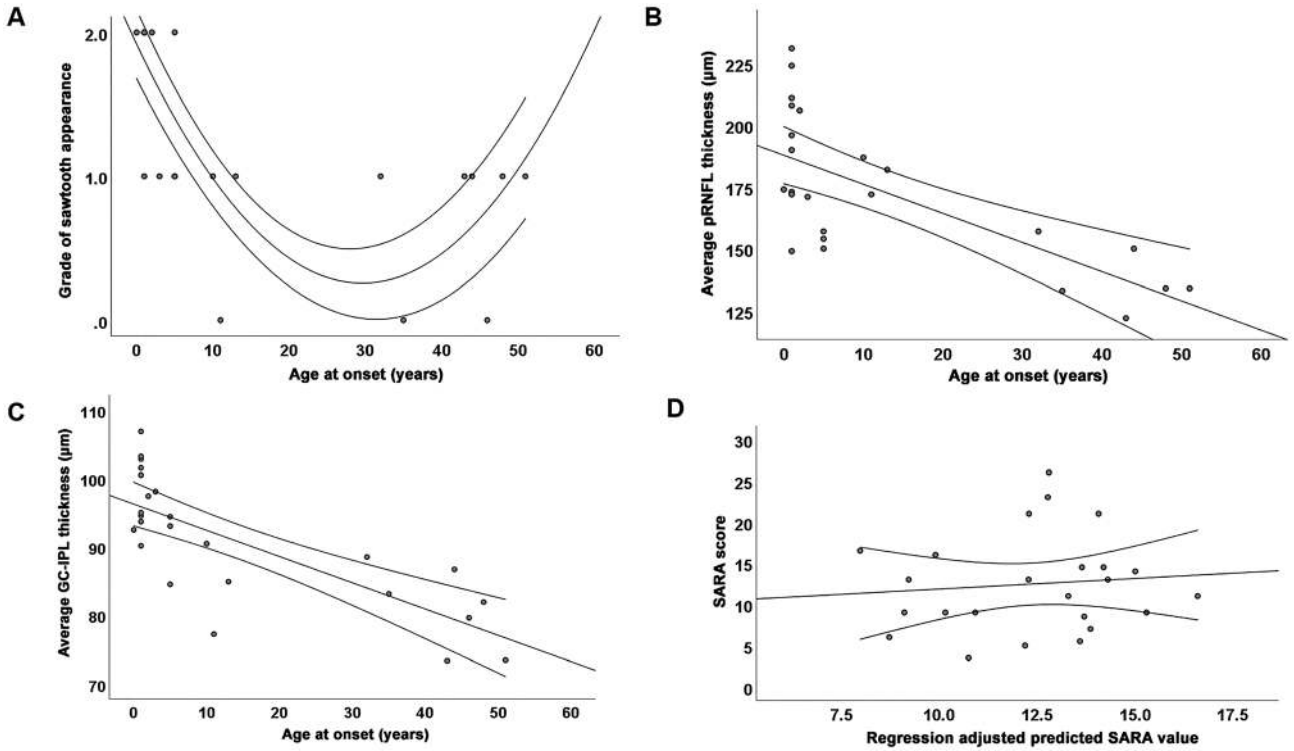

FIG. 3. Correlations between retinal architecture and clinical data in autosomal recessive spastic ataxia of Charlevoix-Saguenay (ARSACS) patients. Ordinal regression plot depicts the correlation between the grade of sawtooth appearance and age at onset (**A**) ($P < 0.05$; $R^2 = 0.607$). Linear regression plots show the associations between: average pRNFL thickness and age at onset (**B**) ($P < 0.05$; $R^2 = 0.491$); average GC-IPL thickness and age at onset (**C**) ($P < 0.05$; $R^2 = 0.591$); and SARA score and predicted SARA score adjusted by age and inferior RNFL thickness (**D**) ($P < 0.05$; $R^2 = 0.01$). pRNFL, peripapillary retinal nerve fiber layer; GC-IPL, ganglion cell-inner plexiform layer; SARA, Scale for the Assessment and Rating of Ataxia.

controls had lower average pRNFL values. This suggests that among patients with hereditary ataxia or SPG, the average pRNFL can diagnose ARSACS with 100% accuracy. Our SD-OCT findings are similar to those reported by Parkinson et al, who found that a time domain OCT (TD-OCT) pRNFL threshold of 119 µm provided a sensitivity of 100% and a specificity of 99.4% in the differentiation between ARSACS and other hereditary ataxias.[6] Our study demonstrates for the first time that SD-OCT is also accurate in distinguishing ARSACS from SPGS. This is important in clinical practice since the neurological phenotypes of these disorders significantly overlap: complicated SPGs often display a combination of spasticity, cerebellar ataxia, and peripheral neuropathy,[26] whereas ARSACS may exhibit isolated pyramidal signs resembling uncomplicated SPGs.[27]

Are the other retinal changes seen in ARSACS "epiphenomena" secondary to thickened RNFL? To answer this, we have evaluated patients with RNFL thickening due to papilledema. Although vascular tortuosity may be seen in both conditions, in our cohort foveal hypoplasia, sawtooth appearance, and papillomacular fold only occurred in ARSACS. When present, peripapillary retinal folds in papilledema are usually annular and not radial. Moreover, macular microcysts in ARSACS occur in both INL and ganglion cell layer (GCL), whereas in papilledema and optic neuropathies they are only found in INL.[28] It seems most of the retinal changes in ARSACS are *primary* abnormalities directly caused by *SACS* mutations.

In healthy subjects FDD inversely correlates with RNFL[21] and macular[22] measurements, but this has not been considered previously in ARSACS. Our ARSACS patients had a significantly shorter FDD when compared to healthy controls. The mean FDD in our ARSACS cohort (3.74 mm) was also 21% less than that reported for a large population-based study with 3468 participants.[29] This will have contributed to the abnormal retinal measurements in ARSACS because a shorter FDD implies less retinal area to accommodate retinal tissue. Indeed, our data show an inverse correlation between FDD and severity of papillomacular fold and sawtooth appearance and total macular thickness. However, FDD does not fully explain the retinal thickening in ARSACS; in our linear regression analysis, all the differences between RNFL and macular layers measurements in ARSACS and controls remained significant after adjusting for FDD.

Our results therefore show that the retinal abnormalities in ARSACS are present in all layers and are not 'epiphenomena' due to thickened RNFL or shortened

FDD. What is the likely mechanism involved? Nethisingue et al proposed that thickened RNFL might be due to abnormal axoplasmic transport in the unmyelinated portion of retinal ganglion cell axons, leading to increased fiber diameter.[14] Another group speculated that axoplasmic stasis and edema could be due to disrupted mitochondrial transport since sacsin localizes to mitochondria.[15] A different mechanism was proposed by Gazulla et al[17] who stated funduscopic changes in ARSACS probably resulted from an increased number of retinal nerve fibers, implying retinal *hyperplasia*. Our study has extended these observations to demonstrate abnormal thickening of *all* the retinal layers, suggesting an excess of all neural tissue in the ARSACS retina. Given the limited retinal area, this excess tissue is likely to have led to a "folding" process, explaining the sawtooth appearance, papillomacular folds, and vascular tortuosity. In support of this concept of hyperplastic retina, tractography in ARSACS revealed thickening in the transverse fibers of the pons, also thought to be due to hyperplasia.[17]

Our youngest ARSACS patient was 16 years old; we are therefore unable to say if these retinal changes are present at birth. However, indirect evidence suggests they are. First, foveal hypoplasia has only ever been described in congenital rather than acquired conditions.[30-33] Second, we found an inverse correlation between age and measurements of retinal layer thickness. Third, in five of our ARSACS cases serial measurements of RNFL thickness for up to 5 years showed no progression. Finally, the FDD in ARSACS is abnormally short; FDD usually increases with age, but only by 11% from infancy to adulthood,[34] so the abnormal FDD in ARSACS is probably lifelong. We therefore propose that the retinal changes seen in ARSACS are congenital and reflect an effect of *SACS* mutations on prenatal retinal development. Interestingly, ganglion cells are the first to differentiate and migrate in developing retina, so failures in this process could create abnormal architecture.[35] In particular, insufficient programmed cell death would result in a greater number of ganglion cells and their axons, implying thicker GCL and RNFL, and provide molecular signals promoting survival of other retinal layers. It is likely that sacsin also has a role in foveal development, which normally involves centrifugal migration of cells from the inner retinal layers creating the foveal depression between 25 weeks of gestation and 15 months of age.[36]

This study has identified quantifiable OCT abnormalities in ARSACS, which might be useful as biomarkers for future clinical trials. OCT measurements are being proposed as biomarkers in Alzheimer's disease, Parkinson's disease, multiple sclerosis, and other neurological conditions.[37] Moreover, RNFL has been shown to correlate with disease severity in Friedreich's ataxia[38] and SCA3.[39] Parkinson et al have demonstrated age at onset inversely correlated with average RNFL in ARSACS.[6] Herein, we found that in addition to pRNFL thickness, macular measurements of RNFL, GC-IPL, INL, and ONL also inversely correlate with age at onset in ARSACS, as do the grades of vascular tortuosity, papillomacular fold, and sawtooth appearance. More importantly, age-adjusted inferior RNFL positively correlated with SARA scores, so this may be the most promising disease progression biomarker in ARSACS.

There are limitations to this study. We could not include all variables likely to influence retinal architecture in ARSACS in a multivariate analysis due to the sample size, and we did not investigate the correlation of retinal measurements with other potential biomarkers such as brain magnetic resonance imaging and neurofilament levels. Furthermore, we only analyzed the right eye of our patients, which reduced statistical power. Maximum OCT follow-up was 5 years, and so data on progression over time are limited.

In conclusion, retinal structure in ARSACS suggests it has a neurodevelopmental pathogenesis. Several of the retinal abnormalities seen on OCT are unique to ARSACS. The association of inferior RNFL thickness with SARA scores suggests OCT may provide relevant disease progression biomarkers for future clinical trials. ■

Acknowledgments: We are grateful to patients and their families for contributing to this research, and to Dr. Jonathan Oakley for providing guidance and technical support in Orion™ software operation. P.G. is supported by the National Institute for Health Research University College London Hospitals Biomedical Research Centre UCLH. P.G. also receives support from the North Thames CRN. P.G. and F.B. work at University College London Hospitals/University College London, which receives a proportion of their funding from the Department of Health's National Institute for Health Research Biomedical Research Centre's funding scheme.

Ethical Statement

Full consent was obtained from the patients or their legal guardians for this study. The project for this research received approval from the authors' local ethics committee.

References

1. Bouchard JP, Barbeau A, Bouchard R, Bouchard RW. Autosomal recessive spastic ataxia of Charlevoix-Saguenay. Can J Neurol Sci 1978;5(1):61–69.
2. Engert JC, Bérubé P, Mercier J, et al. ARSACS, a spastic ataxia common in northeastern Quebec, is caused by mutations in a new gene encoding an 11.5-kb ORF. Nat Genet 2000;24:120–125.
3. Vermeer S, Meijer RPP, Pijl BJ, et al. ARSACS in the Dutch population: a frequent cause of early-onset cerebellar ataxia. Neurogenetics 2008;9(3):207–214.
4. Baets J, Deconinck T, Smets K, et al. Mutations in SACS cause atypical and late-onset forms of ARSACS. Neurology 2010;75(13):1181–1188.

5. Pilliod J, Moutton S, Lavie J, et al. New practical definitions for the diagnosis of autosomal recessive spastic ataxia of Charlevoix-Saguenay. Ann Neurol 2015;78(6):871–886.
6. Parkinson MH, Bartmann AP, Clayton LMS, et al. Optical coherence tomography in autosomal recessive spastic ataxia of Charlevoix-Saguenay. Brain 2018;141(4):989–999. https://academic.oup.com/brain/article/141/4/989/4930786
7. Rezende Filho FM, Parkinson MH, Pedroso JL, et al. Clinical, ophthalmological, imaging and genetic features in Brazilian patients with ARSACS. Parkinsonism Relat Disord 2019;62:148–155.
8. Synofzik M, Soehn AS, Gburek-Augustat J, et al. Autosomal recessive spastic ataxia of Charlevoix Saguenay (ARSACS): expanding the genetic, clinical and imaging spectrum. Orphanet J Rare Dis. 2013;8(41). https://doi.org/10.1186/1750-1172-8-41
9. Desserre J, Devos D, Sautière BG, et al. Thickening of peripapillar retinal fibers for the diagnosis of autosomal recessive spastic ataxia of Charlevoix-Saguenay. Cerebellum 2011;10(4):758–762.
10. Vingolo EM, di Fabio R, Salvatore S, et al. Myelinated retinal fibers in autosomal recessive spastic ataxia of Charlevoix-Saguenay. Eur J Neurol 2011;18(9):1187–1190.
11. Barboni P, Savini G, Valentino ML, et al. Retinal nerve fiber layer evaluation by optical coherence tomography in Leber's hereditary optic neuropathy. Ophthalmology 2005;112(1):120–126.
12. Karam EZ, Hedges TR. Optical coherence tomography of the retinal nerve fibre layer in mild papilloedema and pseudopapilloedema. Br J Ophthalmol 2005;89(3):294–298.
13. Savini G, Bellusci C, Carbonelli M, et al. Detection and quantification of retinal nerve fiber layer thickness in optic disc edema using stratus OCT. Arch Ophthalmol 2006;124(8):1111–1117.
14. Nethisinghe S, Clayton L, Vermeer S, et al. Retinal imaging in autosomal recessive spastic ataxia of Charlevoix-Saguenay. Neuro-Ophthalmol 2011;35(4):197–201.
15. Yu-Wai-Man P, Pyle A, Griffin H, Santibanez-Korev M, Rita Horvath R, Chinnery PF. Abnormal retinal thickening is a common feature among patients with ARSACS-related phenotypes. Br J Ophthalmol 2014;98(5):711–713.
16. Gazulla J, Benavente I, Vela AC, Marín MA, Pablo LE, Tessa A, et al. New findings in the ataxia of Charlevoix-Saguenay. J Neurol 2012;259(5):869–878.
17. Gazulla J, Vela AC, Marín MA, et al. Is the ataxia of Charlevoix-Saguenay a developmental disease? Med Hypotheses 2011;77(3):347–352.
18. de Freitas JL, Rezende Filho FM, Sallum JMF, França MC, Pedroso JL, Barsottini OGP. Ophthalmological changes in hereditary spastic paraplegia and other genetic diseases with spastic paraplegia. J Neurol Sci. 2020;409:116620.
19. Marianelli BF, Filho FMR, Salles MV, et al. A proposal for classification of retinal degeneration in spinocerebellar ataxia type 7. Cerebellum 2020. https://doi.org/10.1007/s12311-020-01215-6
20. Shah CT, Ward TS, Matsumoto JA, Shildkrot Y. Foveal hypoplasia in autosomal recessive spastic ataxia of Charlevoix-Saguenay. J AAPOS 2016;20(1):81–83.
21. Hong SW, Ahn MD, Kang SH, Im SK. Analysis of peripapillary retinal nerve fiber distribution in normal young adults. Invest Ophthalmol Vis Sci 2010;51(7):3515–3523.
22. Qiu K, Wang G, Zhang R, Lu X, Zhang M, Jansonius NM. Influence of optic disc-fovea distance on macular thickness measurements with OCT in healthy myopic eyes. Sci Rep. 2018;8:5233.
23. Cruz-Herranz A, Balk LJ, Oberwahrenbrock T, et al. The APOSTEL recommendations for reporting quantitative optical coherence tomography studies. Neurology 2016;86(24):2303–2309.
24. Tewarie P, Balk L, Costello F, et al. The OSCAR-IB consensus criteria for retinal OCT quality assessment. PLoS One 2012;7(4):e34823.
25. Thomas MG, Kumar A, Mohammad S, et al. Structural grading of foveal hypoplasia using spectral-domain optical coherence tomography: a predictor of visual acuity? Ophthalmology 2011;118(8):1653–1660.
26. Shribman S, Reid E, Crosby AH, Houlden H, Warner TT. Hereditary spastic paraplegia: from diagnosis to emerging therapeutic approaches. Lancet Neurol 2019;18(12):1136–1146.
27. Gregianin E, Vazza G, Scaramel E, et al. A novel SACS mutation results in non-ataxic spastic paraplegia and peripheral neuropathy. Eur J Neurol 2013;20(11):1486–1491.
28. Abegg M, Dysli M, Wolf S, Kowal J, Dufour P, Zinkernagel M. Microcystic macular edema: retrograde maculopathy caused by optic neuropathy. Ophthalmology 2014;121(1):142–149.
29. Jonas RA, Wang YX, Yang H, Li JJ, Xu L. Optic disc-fovea distance, axial length and parapapillary zones. The Beijing Eye Study 2011. PLoS One 2015;10(9):e0138701.
30. McCafferty BK, Wilk MA, McAllister JT, et al. Clinical insights into foveal morphology in albinism. J Pediatr Ophthalmol Strabismus 2015;52(3):167–172.
31. Kondo H. Foveal hypoplasia and optical coherence tomographic imaging. Taiwan J Ophthalmol 2018;8(4):181–188.
32. Hingorani M, Williamson KA, Moore AT, van Heyningen V. Detailed ophthalmologic evaluation of 43 individuals with PAX6 mutations. Invest Ophthalmol Vis Sci 2009;50(6):2581–2590.
33. Kohl S, Zobor D, Chiang WC, et al. Mutations in the unfolded protein response regulator ATF6 cause the cone dysfunction disorder achromatopsia. Nat Genet 2015;47(7):757–765.
34. De Silva DJ, Cocker KD, Lau G, Clay ST, Fielder AR, Moseley MJ. Optic disk size and optic disk-to-fovea distance in preterm and full-term infants. Invest Ophthalmol Vis Sci 2006;47(11):4683–4686.
35. Cepko CL, Austin CP, Yang X, Alexiades M, Ezzeddine D. Cell fate determination in the vertebrate retina. Proc Natl Acad Sci U S A 1996;93(2):589–595. http://www.pnas.org/content/pnas/93/2/589.full.pdf
36. Hendrickson A, Possin D, Vajzovic L, Toth C. Histological development of the human fovea from midgestation to maturity. Am J Ophthalmol 2012;154(5):767–778.
37. Satue M, Obis J, Rodrigo MJ, et al. Optical coherence tomography as a biomarker for diagnosis, progression, and prognosis of neurodegenerative diseases. J Ophthalmol 2016;2016:8503859.
38. Fortuna F, Barboni P, Liguori R, et al. Visual system involvement in patients with Friedreich's ataxia. Brain 2009;132(116):123.
39. Alvarez G, Rey A, Sanchez-Dalmau FB, Muñoz E, Ríos J, Adán A. Optical coherence tomography findings in spinocerebellar ataxia-3. Eye 2013;27(12):1376–1381.

Supporting Data

Additional Supporting Information may be found in the online version of this article at the publisher's web-site.